Wang *et al. Carbon Research* (2024) 3:36
https://doi.org/10.1007/s44246-024-00120-5

Carbon Research

ORIGINAL ARTICLE

Open Access

Efficient reclamation of phosphorus from wetland plant via $CaCl_2$/NaOH-mediated hydrothermal carbonization: insights from the evolution of phosphorus

Junxia Wang[1], Fan Yu[2], Xutong Wang[3], Yuting Wang[4], Zhanjun Cheng[1], Xiaoqiang Cui[1*], Beibei Yan[1] and Guanyi Chen[1,5*]

Abstract

Hydrothermal carbonization (HTC) of wetland plant could achieve the recovery of phosphorus (P) via the production of P-enriched hydrochar to alleviate the crisis of phosphate resources, while the migration and transformation of P should be determined. In this study, *Canna indica* was derived into hydrochar through HTC at different temperatures (200°C-260°C) and liquid mediums (H_2O, $CaCl_2$, and NaOH). The P forms were systematically characterized using P K-edge X-ray absorption near edge structure (XANES), ^{31}P liquid nuclear magnetic resonance (NMR), and sequential extraction. The total P content in hydrochar was up to 23 mg g^{-1} with mainly inorganic P (> 97.8%), and the recovery rate was almost 100% during NaOH-mediated HTC. The P species, monoester-P and soluble orthophosphate (ortho-P), in biomass were transformed to more stable ortho-P in hydrochars, which was highly dependent on temperature and liquid medium. With increasing temperature, Al/Mg-P was gradually replaced by Ca/Fe-P. The $CaCl_2$ solution facilitated the transformation of $Ca(H_2PO_4)_2$ into $CaHPO_4$ by elevating the Ca/P ratio. While for the NaOH-mediated HTC, the $CaHPO_4$ and $Ca(H_2PO_4)_2$ were transformed to hydroxyapatite (74.3%-81.5%), and the proportion of $MgHPO_4$ elevated with increasing temperature. The diffusive gradients in thin films (DGT) results implied that the addition of hydrochar greatly elevated the soil available P content, which was further promoted by high temperature and NaOH medium. These results indicate that the species and availability of P in hydrochar could be adjusted through varying liquid medium and reaction temperature, which provide guidance for the target design of P-enriched hydrochar and P reclamation.

Highlight

- P-enriched hydrochar was prepared from the wetland plant by the modified HTC.
- Liquid medium and reaction temperature affected the speciation dynamics of P.
- P was stabilized with high temperature, Ca^{2+} addition, and alkaline liquid medium.
- Hydrochar addition greatly elevated the soil available P content via DGT analysis.

Handling Editor: Fenchang Wu.

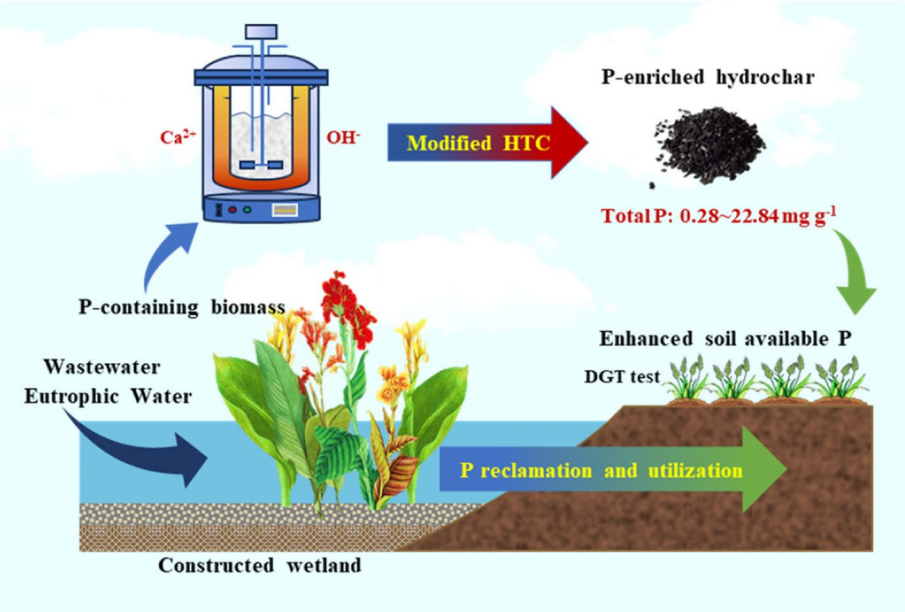
*Correspondence:
Xiaoqiang Cui
cuixiaoqiang@tju.edu.cn
Guanyi Chen
chen@tju.edu.cn
Full list of author information is available at the end of the article

Springer

© The Author(s) 2024. **Open Access** This article is licensed under a Creative Commons Attribution 4.0 International License, which permits use, sharing, adaptation, distribution and reproduction in any medium or format, as long as you give appropriate credit to the original author(s) and the source, provide a link to the Creative Commons licence, and indicate if changes were made. The images or other third party material in this article are included in the article's Creative Commons licence, unless indicated otherwise in a credit line to the material. If material is not included in the article's Creative Commons licence and your intended use is not permitted by statutory regulation or exceeds the permitted use, you will need to obtain permission directly from the copyright holder. To view a copy of this licence, visit http://creativecommons.org/licenses/by/4.0/.

Keywords Hydrothermal carbonization, Phosphorus, Liquid medium, Hydrochar

Graphical Abstract



1 Introduction

Phosphorus (P) is one of the necessary nutrients for plant growth (Vaclav 2000), and effective input of P is urgent in agriculture to secure soil fertility and crop yield. However, phosphate ore, the main feedstock for P fertilizer production, is a non-renewable resource and may be depleted in the coming decades as the demand for P increases (Cui et al. 2020; Hao et al. 2013; Heilmann et al. 2014). Thus, it is necessary to develop P alternative resources. In contrast to the limited terrestrial phosphorus resource, eutrophication of water has been a common issue worldwide (Gorzelnik et al. 2023). According to the 2021 China Ecological Environment Status Bulletin, the proportion of eutrophic lakes and reservoirs in China was up to 27.3%. Therefore, reclaiming excess P from water and applying it to P-deficient soils would be an appropriate strategy to achieve both the restoration of eutrophic water and the alleviation of the pressure from P deficiencies. The constructed wetland is an inexpensive and environmental-friendly water remediation technology that is widely used for the efficient removal of P from eutrophic water and wastewater (Ge et al. 2019). However, the operation of the constructed wetlands could produce a large amount of wetland plant (WP) waste. According to the 2nd National Wetland Resources Investigation, China's constructed wetland area is 6.75 million hectares, which could generate about 107 Mt of WP biomass annually (Cui et al. 2016). It is necessary to regularly harvest and dispose of WP to prevent the residues from decaying and releasing phosphorus into the water, which causes secondary pollution. Compared to the total P (0.08–4.62 mg g^{-1}) in general agricultural residues, grass, and wood (Yang et al. 2021), the WP contained more P (2.6–8.9 mg g^{-1}) (Cui et al. 2020, 2019; Liu et al. 2011). However, the water-soluble phosphorus was the main form in WP, and the direct application has a potential risk of P leaching (Cui et al. 2020; Yu et al. 2022). Thus, it is crucial to explore and design a reasonable process of WP resource utilization for the industrialization of artificial eco-wetlands. The appropriate utilization of these P-enriched WP is essential to prevent secondary pollution and to achieve P recovery from water.

Biochar, a carbon-rich solid, is obtained from pyrolysis of biomass under oxygen-limited conditions (Kambo and Dutta 2015). It has gained much attention in recent years due to its potential for soil improvement and increasing crop yields (El-Naggar et al. 2019). Growing focus has been given to the role of biochar in the soil P cycle (El-Naggar et al. 2019; Tan and Lagerkvist 2011).

Traditional pyrolysis (Kambo and Dutta 2015) and torrefaction (Yek et al. 2021) technologies require biomass with low moisture content, while wetland plants have high moisture content, resulting in increased energy consumption. Noteworthy, wet thermochemical treatments such as hydrothermal carbonization (HTC) and wet torrefaction have demonstrated significant potential in terms of energy efficiency and environmental sustainability (Osman et al. 2023). Wet torrefaction is conducted under normal pressure with the merit of low cost, and HTC requires a short residence time with the generation of valuable hydrochar (Akbari et al. 2020; Babinszki et al. 2020). Therefore, HTC emerged as a promising technique for the treatment of biomass waste with high moisture content, as well as the production of hydrochar. Previous study showed that the hydrochar derived from WP had a P content exceeding 20 mg g^{-1} (Cui et al. 2020), surpassing that of biochar derived from wood (0.14–0.60 mg g^{-1}), grass (0.59–4.73 mg g^{-1}), and general crop straw (1.2–16.6 mg g^{-1}) (Robinson et al. 2018; Sun et al. 2018; Xu et al. 2016; Yang et al. 2021). However, the migration of P to the liquid product was evident during HTC (Cui et al. 2019). Compared to the high recovery of P in pyrolysis biochar, the recovery of P in hydrochar was less, with approximately 60% for microalgae (Ekpo et al. 2016b), 30–80% for *Napier grass* (Cui et al. 2019), and little for distiller's grains at 200°C (Heilmann et al. 2011b). The efficient P enrichment on hydrochar is the key to achieving P resource recovery during the HTC.

Current studies have shown that the recovery of P in hydrochar during HTC is influenced primarily by the nature of the feedstock and reaction conditions, such as temperature, residence time, and liquid phase medium (Chen et al. 2022; Ekpo et al. 2016a, 2016b; Ghanim et al. 2018; Heilmann et al. 2011a; Huang et al. 2018; Huang and Tang 2016). Organic P (phytic acid and monoester phosphorus) and polyphosphate in solid waste could be converted to orthophosphate by hydrolysis after HTC treatment (Chen et al. 2022). Insoluble phosphates could be formed owing to the presence of metal cations such as calcium (Ca), aluminum (Al), iron (Fe), and magnesium (Mg) in the feedstock, which would contribute to the fixation of the P in hydrochar. Animal manures had a higher metal content (2.6–5.1%) (Heilmann et al. 2011a, 2011b) than microalgae and distiller's grains (< 0.5%) (Heilmann et al. 2014), which led to the fact that manure derived hydrochar was the primary P enrichment product, whereas almost all P from microalgae and distiller's grains were concentrated in liquid products. The recovery of P in the sewage sludge-derived hydrochar increased to 95% with the addition of $CaCl_2$, and more P was retained as Ca-P in hydrochar (Zheng et al. 2020). Besides, the pH of the liquid-phase medium has a significant effect on the migration and transformation of P during the HTC process. The addition of 0.1 M H_2SO_4 to swine manure in HTC treatment resulted in 80% P recovery in the liquid product, while 87–95% P recovery in hydrochar was achieved with the addition of NaOH, CH_3COOH and HCOOH (Ekpo et al. 2016a). The low pH could inhibit the reaction of metals with P to form insoluble P thereby reducing the solid-phase recovery of P (Zheng et al. 2020). The temperature of HTC affects P conversion and recovery as well. However, the effect of temperature on the solid-phase P recovery from hydrochar varied with feedstock properties. The relationships between the HTC temperature and P recovery for the poultry manure, pig manure, and cow manure were non-correlated, significant positive correlated, and weak positive correlated, respectively (Heilmann et al. 2014). Similarly, the effect of HTC temperature on P recovery from WP derived hydrochar varied with the species (Cui et al. 2020). Hence, the efficient P enrichment on hydrochar is expected to be achieved through regulating the key HTC parameters, such as liquid phase medium and temperature, and the migration and speciation mechanism of P during the HTC process is imperative for the targeted reclamation of P.

In addition to the changes in P during HTC, the changes in soil P after the application of hydrochar to the soil are worthy of note. Contributions of available P to the soil after hydrochar application are controlled by both endogenous P and extraneous soil media (Prendergast-Miller et al. 2014; Qian et al. 2013; Yang et al. 2021). Nevertheless, the role of intrinsic P in biochar in influencing soil P cycling received little attention. At present, the determination of available P content in soil has been done mostly by chemical leaching, which cannot reflect the actual soil conditions, or model dynamically the supply process of P from the solid phase to soil solution after application (Yang et al. 2021). Unlike the leaching method, the gradient diffusion in thin film (DGT) technique can simulate the dynamic process of P in the ambient medium under in situ conditions (Li et al. 2019), which is based on the principle of free diffusion and can accurately assess the biological effectiveness of P and can better predict the plant response to P (Heidari et al. 2017).

In this study, *C. indica*, a typical wetland plant was selected as feedstock for the production of hydrochars at different temperatures (200–260°C) and liquid media (H_2O, NaOH, and $CaCl_2$ solutions) to achieve the efficient recovery of P. The P speciation in *C. indica* and the derived hydrochars were analyzed in detail by P K-edge X-ray absorption near edge structure (P-K edge XANES), ^{31}P liquid nuclear magnetic resonance (^{31}P NMR) spectroscopy and sequential chemical extraction. The DGT

technology was employed to explore the availability of P in the soil after hydrochar application. The main objective of this study was to achieve the efficient recovery of P from WP via the HTC under different temperatures and reaction media, with special emphasis on the migration mechanisms of P under different liquid media and the effect of hydrochar addition on soil available P.

2 Materials and methods

2.1 Materials and hydrothermal treatments

The *C. indica* (CI) was collected from the constructed wetland in Tianjin, China (38°55′58″ N, 117°41′58″ E). After being washed and air-dried for one week, the harvested biomass was chopped into about 3 cm pieces. The chopped sample was dried at 80°C and ground into powder smaller than 0.45 mm by a pulverizer (YK-1000 A, China).

Hydrothermal carbonization was carried out in a high-pressure stirred reactor (MMJ-200, Japan). Hydrochar was prepared by mixing 10.0 g of CI with 100.0 mL of deionized water. In contrast, 1 M NaOH solution and 0.015 M $CaCl_2$ solution were substituted for deionized water in the hydrothermal process. After sealing the reactor, nitrogen (N_2) was applied to purge air, and the stirring speed was set to 120 rpm. The hydrothermal reaction was conducted at the preset temperatures of 200°C, 220°C, 240°C, and 260°C, respectively, and sustained the peak temperature for 120 min. Then, the reactor was cooled naturally to room temperature. The solid residue (i.e., hydrochar) was collected by filtration and dried at 105°C to a constant weight. The dried hydrochar was weighed and ground to pass through a 0.25 mm stainless steel sieve. The liquid products were kept frozen at -20°C for further analysis. The derived hydrochar was denoted as Liquid Solvent-Hydrothermal temperature (i.e., WH200-260, CH200-260, and NH200-260).

2.2 P K-edge XANES analysis

The P-K edge XANES spectra were measured at Beijing Synchrotron Radiation Facility (BSRF) Line 4B7A of Intermediate Energy Station. Twelve phosphorus-containing compounds were selected for the phosphorus standard samples, namely aluminium phosphate ($AlPO_4$), ferrous phosphate ($FePO_4$), magnesium hydrogen phosphate ($MgHPO_4$), calcium hydrogen phosphate ($CaHPO_4$), monocalcium phosphate ($Ca(H_2PO_4)_2$), calcium phosphate tribasic ($Ca_3(PO_4)_2$), hydroxylapatite (HAP), octacalcium phosphate (OCP), tripotassium orthophosphate (K_3PO_4), potassium dihydrogen phosphate (KH_2PO_4), dipotassium hydrogen phosphate (K_2HPO_4), and phytic acid sodium. The biomass and its derived hydrochars were ground into fine powder. The above standard and test samples were blown uniformly onto phosphorus-free Kapton tape with thin films formed. The XANES data were collected in fluorescence mode with a scanning range of 2120–2200 eV. An iterative linear combination fit (LCF) was performed on the XANES spectra to derive the most probable forms of phosphorus in the samples, and the residual factor (*R*-factor) was used to assess the goodness of fit, where the fit with the smallest *R*-value was considered to be the best fit.

2.3 ^{31}P NMR spectroscopy analysis

The extraction of 0.8 g sample was performed with 20 mL of 0.05 M EDTA-0.25 M NaOH solution at 25 °C for 16 h, followed by centrifugation and filtration. To determine the extraction efficiency, 2 mL of the filtrate was taken to measure the P content. Then, the remaining filtrate was freeze-dried and 0.3 g of the lyophilized powder was redissolved in 0.1 mL of 1 M NaOH and 0.6 mL of D_2O. The sample was completely mixed before centrifugation for NMR analysis. A 400 NMR spectrometer (Bruker Avance III) was used to measure the ^{31}P NMR spectra of the supernatant at 162 MHz. NUTS software was applied to calculate the relative abundance of P species and the area integration of ^{31}P NMR spectra of EDTA-NaOH extracts was performed.

2.4 Extraction and chemical analysis of phosphorus

In this study, H_2SO_4-H_2O_2 digestion, sequential extraction analytical, and ammonium molybdate spectrophotometry were applied to determine the different forms of P content in the biomass and the derived hydrochars. Total P (TP) in the samples was determined by ammonium molybdate spectrophotometry after pre-digestion treatment with H_2SO_4-H_2O_2, while inorganic P (IP) content was determined by 1 M HCl extraction for 16 h. Organic P (OP) content was determined by calculating the difference between TP and IP. The derived liquid product from HTC was digested with potassium persulfate and then TP was determined by spectrophotometry.

The different P forms of the feedstock and the derived hydrochars were analyzed by a modified sequential chemical extraction procedure. In this experiment, 0.2 g of sample was extracted sequentially with 30 mL of deionized water, 0.5 M $NaHCO_3$, 0.1 M NaOH, and 1 M HCl and then shaken at 25 °C for 16 h. After centrifugation and filtration, the P concentration was determined with a UV spectrophotometer (UV-6000PC, METASH). The four forms of P were corresponding to H_2O-P, $NaHCO_3$-P, NaOH-P and HCl-P, and the P content of the solid residue after extraction was called Res.-P. The analysis of all treatments was performed in triplicate.

The recovery of TP from hydrochars after HTC was calculated by Eq. (1):

$$R = \left(\frac{P_{HC}}{P_{FS}} * Y\right) * 100\% \quad (1)$$

where P_{HC} is the TP content in the hydrochars, P_{FS} is the TP content in the feedstock, and Y represents the yield of hydrochars.

2.5 Characterization of hydrochars

The yield of hydrochar is the ratio of the derived solid product to the feedstock biomass. Ash content was determined by heating the samples in a muffle furnace at 750°C for 5 h. The pH of hydrochars was measured with a pH meter (PHS-3C, Lei-ci) at a fixed mass/volume ratio of 1:20 for hydrochar to deionized water (Inyang et al. 2010). The elemental compositions (considering C, H, N, and S) of the samples were determined by an elemental analyzer (Flash-EA112, Thermo), and the O content was calculated by mass balance. After being digested by mixed acid solution, K, Ca, Na, Mg, Fe, and Al contents in the hydrochars were measured by inductively coupled plasma mass spectrometer (ICP-MS, Agilent 7500a). The information on the surface functional groups of the samples was analyzed by Fourier transform infrared spectra (FTIR, IRAffinity-1S) at 2 cm^{-1} resolution in the range of 500 cm^{-1}–4000 cm^{-1}.

2.6 DGT analysis

The changes in the available P content of soils after hydrochar additions were investigated by the diffusive gradient in thin film (DGT) technology. The ZrO-Chelex (DC/F-Z-05) DGT device used in the study was purchased from Nanjing ZhiSense Environmental Technology Co. The soils were collected from a farm in Tianjin, China. The maximum water holding capacity and TP content of the soil were 43.73% and 1.28 mg g^{-1}, respectively. In this study, 10 g of air-dried soil sample was taken as a blank control treatment and 3% of the hydrochars was mixed in each experimental treatment. After that, ultra-pure water was added to the mixed soil samples to approximately 80% of the maximum field capacity. The samples were mixed thoroughly and kept at 25°C for 48 h. Subsequently, the treated soil was placed in the inner cavity of the DGT device with a clean plastic spoon, so that the soil was in contact with the exposed surface of the DGT device. The soil was added until the inner cavity was filled (about 6 g). The filled DGT device was transferred to a self-sealing bag with a little deionized water, and the bag was kept semi-closed. After 24 h of deployment at 25°C, the DGT device was removed and the surface was cleaned with ultrapure water. The device was separated to place the adsorption layer into 10 mL of 1 M NaOH for 24 h, and the P content of the extract was determined by molybdenum antimony ammonium spectrophotometry. The available P content of the soil determined by the DGT device was calculated based on the above P concentration and the DGT device sample parameters. The DGT-P concentration was calculated as described in the Supporting Information.

2.7 Statistical analysis

Statistical analysis was performed using SPSS 25.0. A one-way analysis of variance (ANOVA) was performed to compare two factors (temperature and liquid medium) that affected the characteristics and P speciation in the hydrochar. The Tukey HSD was used to test for significant differences among the corresponding index means. Pearson coefficient was used to analyze the correlation ($p < 0.01$). Figures were plotted by Origin 2023.

3 Results and discussion

3.1 Enrichment of P in hydrochars during HTC

3.1.1 P content in the hydrochars

The content of total phosphorus (TP) inorganic phosphorus (IP) and organic phosphorus (OP) in pristine biomass was 2.70 mg g^{-1}, 2.19 mg g^{-1} and 0.51 mg g^{-1}, respectively. The TP content in the hydrochars produced with deionized water (WHs) rose from 0.28 mg g^{-1} to 6.96 mg g^{-1} with increasing temperature ($F = 6492.0$, $p < 0.01$), and that in $CaCl_2$-modified hydrochar (CHs) and NaOH-modified hydrochar (NHs) elevated from 2.62 and 7.31 mg g^{-1} to 7.01 and 22.84 mg g^{-1} ($F_{CHs} = 4615.1$, $p < 0.01$; $F_{NHs} = 4266.3$, $p < 0.01$). The TP content in NH260 was up to 22.84 mg g^{-1}, which was much higher than that in the biochar derived from wood (0.14–0.60 mg g^{-1}), grass (0.59–4.73 mg g^{-1}), and general crop straw (1.2–5.6 mg g^{-1}) (Robinson et al. 2018; Sun et al. 2018; Xu et al. 2016). Polymer hydrolysis and P precipitation formation may account for P accumulation in high-temperature-derived hydrochar (Cui et al. 2020; Dai et al. 2015; Ekpo et al. 2016b). The TP content in the hydrochars showed a trend of NH > CH > WH at the same HTC temperature. In comparison with the deionized water medium, the alkaline condition facilitated the conversion of P to various precipitates during HTC process (Zheng et al. 2020), and the presence of Ca^{2+} in the $CaCl_2$ medium made it easier to reach the saturation of Ca-P crystallization. Additionally, as shown in Fig. 1, the IP fraction of hydrochar accounted for 82.1–99.7% of the TP content, especially for NHs (≥ 97.8%), which was higher than the pristine biomass (81.1%). The results suggested that the HTC process exhibited a preference for the decomposition of OP, which was further enhanced by the presence of metal ions Ca^{2+} and NaOH. Consequently, this led to an elevation in the content of IP in hydrochar, aligning with previous findings (Cui et al. 2020; Zheng et al. 2020).

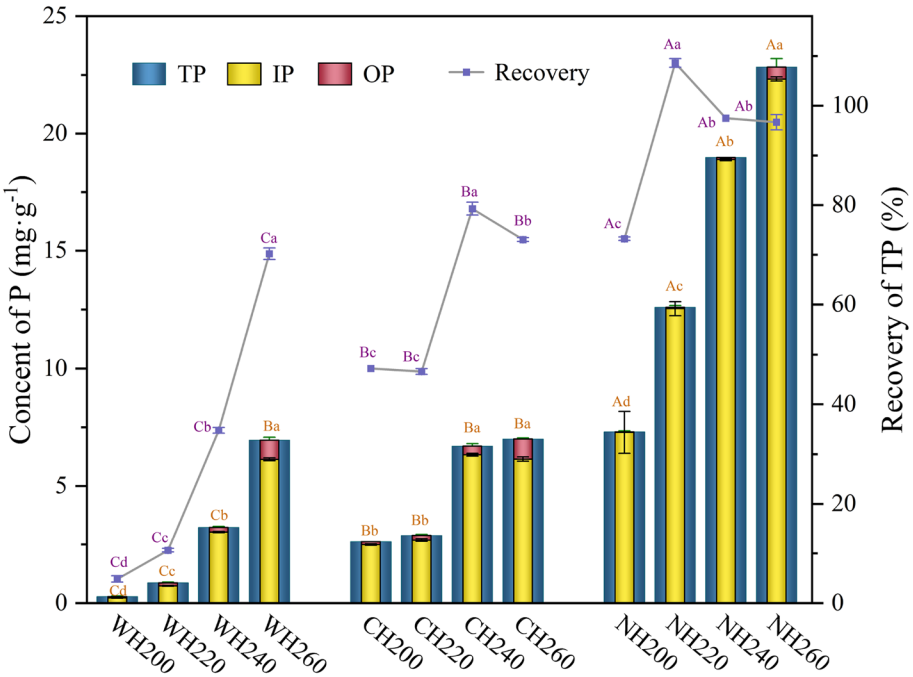


Fig. 1 The recovery and content of P in the hydrochars derived at different temperatures and reaction media. Hydrochars prepared with deionized water, $CaCl_2$ solution, and NaOH solution as the liquid media at different temperatures were represented as WHs, CHs, and NHs, respectively. Error bars represent standard deviation observed for triplicate experiments. Different lowercase letters on the column indicate significant differences among different treatments in the same reaction medium, and different capital letters indicate significant differences among different treatments in the same reaction temperature ($P < 0.01$)

3.1.2 Effect of temperature and liquid medium on the recovery of P in hydrochars

As shown in Fig. 1, the TP recovery rate of NHs was the highest, up to 73.22–108.59%, followed by CHs with 47.22–79.27%, and only 4.87–70.20% of P was recovered in WHs. The recovery of TP varied with different HTC temperatures and liquid medium. The TP recovery of WHs and CHs was significantly associated with the rise of temperature ($r_{WHs} = 0.957$, $p < 0.01$; $r_{CHs} = 0.832$, $p < 0.01$). Similarly, the recovery of P from microalgae, manure and digestate in the liquid product was shown to decrease with increasing temperature (Ekpo et al. 2016b). As for the HTC of wetland plants, previous study reported that the TP recovery of *Napier Grass* increased with increasing temperature, while the recovery of *H. verticillata* and *M. spicatum* was mainly dependent on the feedstock rather than temperature ($F = 2.1$, $P = 0.20$) (Cui et al. 2020, 2019). However, the TP recovery of NHs was not significantly correlated with the HTC temperature in this study ($r = 0.514$, $P = 0.087$). Hence, the increase in temperature had an impact on P retention in hydrochar, but it varied depending on the HTC liquid medium and feedstock. The TP recoveries of WHs and CHs produced at lower temperatures (200–220 °C) were lower than 50%. It indicated that the lower temperature diverted most of the P to the liquid product, which was consistent with previous studies (Cui et al. 2019). As the temperature increased, polymer cleavage occurred and the conversion of organic phosphorus to orthophosphate was more complete, resulting in a significant increase in TP recovery and facilitating P accumulation in solid product (Dai et al. 2015). It was found that the TP recovery of the NHs prepared at higher temperatures (220–260°C) varied from 97–109%, indicating that most of the P was enriched in the hydrochar with the presence of NaOH during HTC process. Previous study found that the P recovery of sludge-derived hydrochar increased from 78 to 91% when the pH was varied from 3 to 13 (Zheng et al. 2022). These results imply that higher reaction temperature and alkaline reaction medium are favorable for P retention in the solid product during HTC.

Notably, as described in Fig. 1, the recovery of TP at the same temperature showed significant differences between the different mediums ($r_{200} = 0.991$, $p < 0.01$; $r_{220} = 0.988$, $p < 0.01$; $r_{240} = 0.972$, $p < 0.01$; $r_{260} = 0.908$, $p < 0.01$, respectively). After HTC treatment, the organic P in solid waste could be turned into orthophosphate (ortho-P) by hydrolysis (Chen et al. 2022; Huang and Tang 2016). The liquid conditions of HTC provided sufficient contact of P with metal cations. In addition, the

initial ortho-P in the feedstock and the generated ortho-P would interact with endogenous or applied cations to form fresh inorganic P species via precipitation or adsorption to be enriched in the hydrochar. As shown in Table 1, the total contents of metals such as Ca, Mg, Fe, and Al in hydrochars produced by different media varied from 19.92- 27.18 mg g^{-1} (WHs), 29.44–37.15 mg g^{-1} (CHs) and 40.06–118.90 mg g^{-1} (NHs), respectively. The dissolution and formation of more stable species during HTC resulted in an increase in the content and recovery of P in hydrochars (Huang et al. 2018). For $CaCl_2$-mediated HTC, Ca^{2+} enhanced the precipitation of P to form insoluble phosphates. These phosphates existed in colloidal form or attached to the hydrochar by electrostatic interaction, which strengthened the enrichment of P in the hydrochars. The recovery of TP was greatly improved. During the HTC of sewage sludge, the addition of calcium caused most of the free P in the process water to be immobilized in the hydrochar (Zheng et al. 2020). In addition to temperature and Ca^{2+}, pH had a significant impact on the migration transformation of P between solid and liquid products as well as the recovery of TP during the HTC process. Higher pH inhibited the migration of P to the liquid products and promoted the precipitation of P with cations, which dramatically improved the TP recovery in hydrochar (Zheng et al. 2020).

As mentioned above, the recovery of P in hydrochar significantly depended on the liquid medium ($F=32.2$, $p<0.01$) instead of temperature ($F=2.8$, $p=0.057$). Higher HTC temperatures, $CaCl_2$, and NaOH liquid medium were favorable to enhance the enrichment of P and improved the recovery of TP in hydrochar, and the alkaline modification showed the greatest improvement. In addition, higher HTC temperature, the addition of Ca^{2+}, and alkaline modification were also beneficial to the enhancement of IP content in hydrochar.

3.2 Transformation of P during HTC

3.2.1 P K-edge XANES spectrum analysis

The forms of phosphorus in *C. indica* and the derived hydrochars were determined by P K-edge XANES. The XANES spectra of phosphorus and the linear superposition fitting (LCF) results in different phosphorus forms and relative abundances were shown in Figs. 2 and 3. The *R*-factor and $\chi 2$ of XANES spectral LCF were presented in Table S1. According to the fitting results, the main phosphorus compounds in *C. indica* were $Ca(H_2PO_4)_2$, K_3PO_4, $AlPO_4$, $CaHPO_4$, and $FePO_4$. After HTC treatment, K_3PO_4 was not detected in the derived hydrochars, while $MgHPO_4$ and hydroxyapatite (HAP) appeared. This indicated that the soluble inorganic phosphates in the biomass were transferred to the liquid phase and combined with metal ions such as calcium, magnesium, and iron to form more stable insoluble phosphate in the hydrochars during the HTC process (Han et al. 2019; Huang et al. 2018). The dissolution and recrystallization of phosphate during the HTC process were greatly affected by liquid medium and reaction temperature.

$AlPO_4$, $CaHPO_4$, $Ca(H_2PO_4)_2$, $FePO_4$, and $MgHPO_4$ were the main P species in WH200. With increasing HTC temperature to 240 and 260°C, $CaHPO_4$, $Ca(H_2PO_4)_2$, and $FePO_4$ became the dominant compounds with the elimination of $AlPO_4$ and $MgHPO_4$, and the corresponding proportion varied with the reaction temperature. Moreover, high Mg content favored

Table 1 The metal concentrations of *C. indica* and the derived hydrochars at different temperatures and reaction media

Sample	Ca	Mg	Fe	Al	Na	molar ratio			
	(mg g^{-1})					Ca/P	Mg/P	Fe/P	Al/P
CI	8.36 ± 0.11	7.06 ± 0.09	0.68 ± 0.03	0.39 ± 0.01	7.78 ± 2.71	2.40	3.38	0.14	0.17
WH200	13.58 ± 0.20	8.32 ± 0.01	1.52 ± 0.16	0.54 ± 0.01	1.64 ± 0.12	37.59	38.38	0.31	0.23
WH220	15.12 ± 0.35	2.84 ± 0.01	1.23 ± 0.09	0.73 ± 0.02	1.57 ± 0.00	13.47	4.22	0.25	0.31
WH240	16.75 ± 0.45	4.73 ± 0.13	1.28 ± 0.00	0.93 ± 0.03	1.59 ± 0.10	4.01	1.89	0.26	0.40
WH260	14.01 ± 0.07	10.05 ± 0.27	1.85 ± 0.06	1.27 ± 0.02	1.50 ± 0.03	1.56	1.87	0.38	0.54
CH200	25.57 ± 0.86	4.62 ± 0.09	1.44 ± 0.07	0.68 ± 0.02	1.74 ± 0.02	7.56	2.28	0.30	0.29
CH220	23.92 ± 0.68	3.27 ± 0.03	1.46 ± 0.13	0.79 ± 0.01	1.75 ± 0.01	6.39	1.46	0.30	0.34
CH240	26.98 ± 0.01	6.88 ± 0.01	2.14 ± 0.26	1.15 ± 0.02	1.53 ± 0.03	3.12	1.33	0.44	0.49
CH260	22.52 ± 0.19	8.75 ± 0.11	1.61 ± 0.29	1.12 ± 0.03	1.46 ± 0.03	2.49	1.61	0.33	0.48
NH200	18.33 ± 0.02	19.07 ± 0.39	1.53 ± 0.06	1.13 ± 0.00	43.35 ± 1.03	1.94	3.37	0.31	0.48
NH220	32.84 ± 0.16	34.74 ± 0.18	2.99 ± 0.05	2.18 ± 0.07	17.94 ± 1.28	2.02	3.56	0.61	0.93
NH240	49.00 ± 0.21	51.65 ± 0.28	4.12 ± 0.01	2.95 ± 0.09	34.93 ± 0.57	2.00	3.51	0.84	1.25
NH260	53.30 ± 0.07	56.60 ± 0.07	5.50 ± 0.65	3.50 ± 0.00	25.97 ± 0.69	1.81	3.20	1.13	1.49

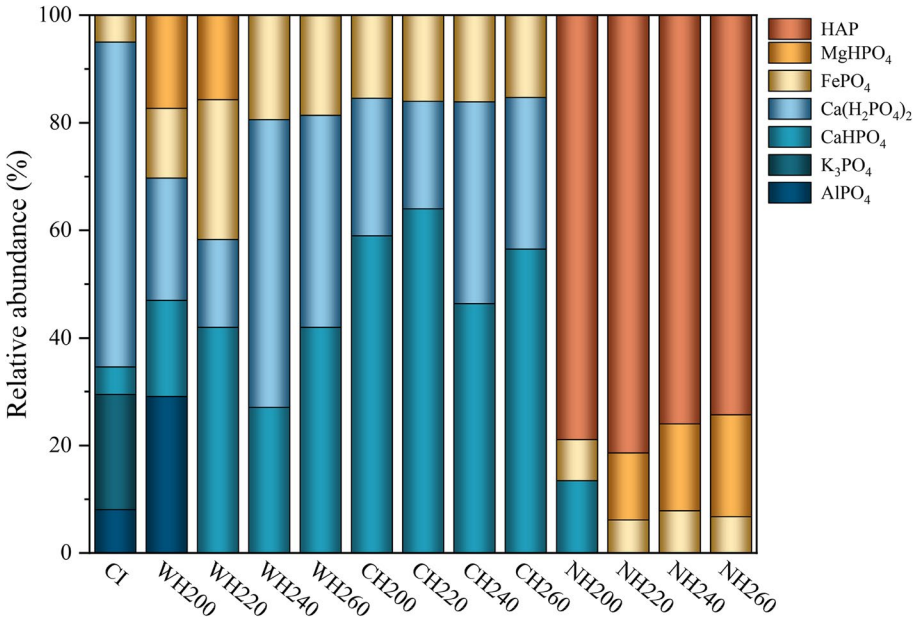


Fig. 2 Relative abundances of different P species in *C. indica* and the derived hydrochars at different temperatures and reaction media, as quantified by linear combination fitting of their XANES spectra

the production of $MgHPO_4$, while high P content preferred that of $MgPO_4$ (Chen et al. 2021). With increasing temperature, the Mg/P of WHs gradually decreased (37.6–1.6) and the pH gradually increased (5.1–6.8), which led to the disappearance of $MgHPO_4$ and $AlPO_4$. Similar to the WHs, $CaHPO_4$, $Ca(H_2PO_4)_2$, and $FePO_4$ were the major P species in the $CaCl_2$ modified hydrochars (CHs), and relative abundance of $CaHPO_4$ and $Ca(H_2PO_4)_2$ were up to 46.4–64.0% and 20.0–37.5%, respectively. However, the proportion of $CaHPO_4$ in CHs was higher than that in WHs (17.9–42.0%) at the same HTC temperature. This indicates that the addition of $CaCl_2$ promoted the transformation of $Ca(H_2PO_4)_2$ to $CaHPO_4$ owing to the increase in Ca/P ratio. Verma and Murugavel have shown that the Ca/P ratio of 1:1 facilitates the production of $CaHPO_4$ compared to 1:2 (Verma and Murugavel 2020). Moreover, the acidic liquid medium also favored the formation of $CaHPO_4$ (Zheng et al. 2020). While for the NaOH-mediated HTC process, the main P species was HAP with a high proportion of 74.3%-81.5%, and no $CaHPO_4$ and $Ca(H_2PO_4)_2$ was detected in the NHs derived at high temperatures (> 200°C), implying that the $CaHPO_4$ and $Ca(H_2PO_4)_2$ were transformed to HAP under alkaline condition during HTC process. Previous study reported that Ca-P complexes could be transformed into thermodynamically preferred HAP during the HTC of sludge (Zheng et al. 2020), which was consistent with the results of this study. Similarly, HAP-P accounted for 48.4–75.5% of the total P content in the hydrochars derived from animal manure (Huang et al. 2018). Generally, high proportion of HAP required high reaction temperature during pyrolysis or incineration (Huang et al. 2018; Huang and Tang 2016), and the NaOH-mediated HTC could greatly promote the formation of HAP with lower energy consumption as compared with the abovementioned dry thermal techniques. Additionally, $MgHPO_4$ (0–18.9%) and $FePO_4$ (6.2–7.9%) were detected in the NHs, and the formation of $MgHPO_4$ was enhanced by high HTC temperature.

XANES spectra showed that Ca-P was the dominant P compound in the *C. indica* biomass and the derived hydrochars. As confirmed by LCF results, Ca-P accounted for 65.5% of the total P content in the feedstock and 40.6–92.4% for the hydrochars. It is noteworthy that the Ca-P proportion of NHs even reached 74–92%, which was much higher than that of hydrochars derived from sewage sludge (13–32%) (Huang and Tang 2016) and animal manure (63.1–75.5%) (Huang et al. 2018). In addition to high Ca content in biomass (Table 1), high temperature and alkaline medium favored the synthesis of Ca-P compounds as well. High homogeneous Ca-P content in the *C. indica* derived hydrochars is beneficial to the further reclamation of P resource. Moreover, the type and concentration of the metal as well as the pH of the liquid medium significantly determined the affinity of phosphorus to metal cations, and the combination of P with Ca or Mg

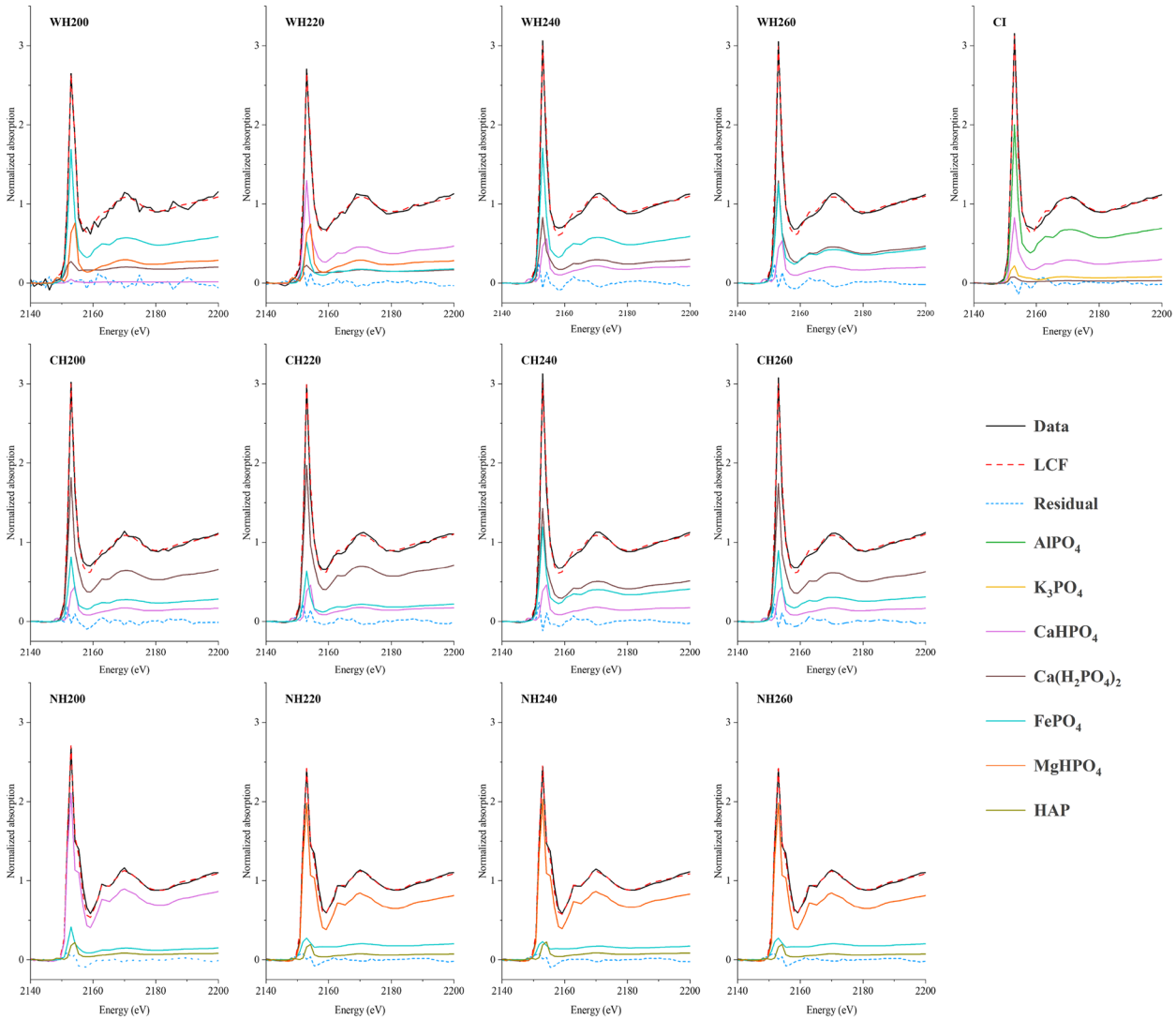


Fig. 3 Linear combination fittings of XANES spectra of *C. indica* and derived hydrochars at different temperatures and reaction media

was particularly facilitated by increasing HTC temperature, adding Ca^{2+}, and alkaline liquid medium.

3.2.2 Speciation of P in hydrochars

^{31}P liquid NMR was employed to determine the P forms in *C. indica* biomass and the derived hydrochars. In this study, the TP content extracted by EDTA-NaOH was between 0.2–13.0 mg g^{-1} and the TP recovery was 47.2–99.6% as shown in Table S2. With the increase in HTC temperature, the extraction efficiency of hydrochar modified by NaOH decreased significantly from 99.6% to 47.2%. The relatively low P extraction rate was possibly attributed to the existence of P in a compact and unextractable form (Xu et al. 2016). As depicted in Fig. 4, orthophosphate (ortho-P, ~5.6 ppm) and monoester-P (4–5 ppm) were detected. Incidentally, the peak of ortho-P was weak in WH200 owing to the little P content (0.2 mg g^{-1}) in the extract solution. The major P species in *C. indica* were ortho-P (92.50%) and monoester-P (7.50%), while monoester-P was not identified in the hydrochars, suggesting that most of the P was transformed to ortho-P during HTC process. Similarly, the conversion of organic phosphates to orthophosphate occurred during the HTC of animal manure (Huang et al. 2018). The elimination of monoester-P peak in all hydrochars indicates that some organic P species in biomass were easily decomposed during HTC process (Cui et al. 2020; Huang and Tang 2016). As shown by ^{31}P NMR spectra, there was no significant difference in the species of phosphorus among the hydrochars derived at different

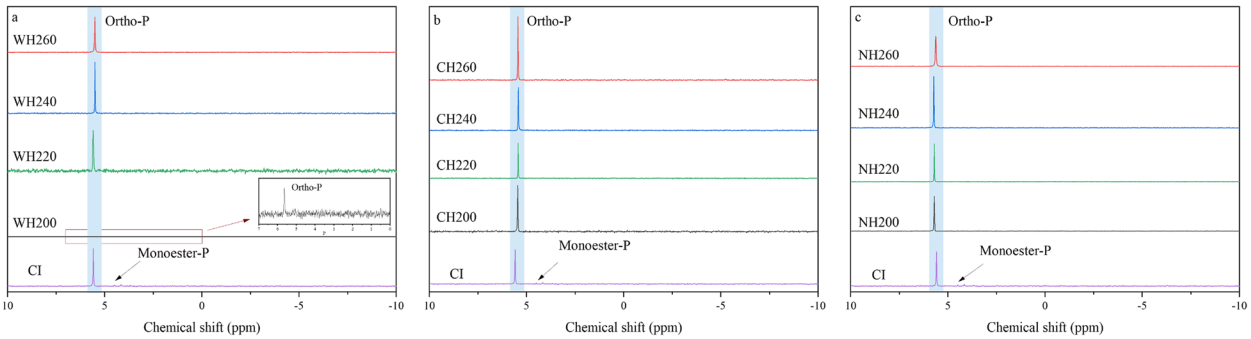


Fig. 4 ^{31}P NMR spectra of *C. indica* and the derived hydrochars at different temperatures and reaction media (**a**) H_2O, (**b**) $CaCl_2$ and (**c**) NaOH

temperatures and liquid mediums, all of which were orthophosphates, corroborated mutually with P-XANES spectra. As distinct from the biochar derived from WP, pyrophosphate was not found in the hydrochar in the present study, which may be attributed to the presence of liquid during HTC allowing for a more complete conversion of P (Cui et al. 2019; Yu et al. 2022).

3.2.3 Sequential extraction and chemical speciation of P

The percentages of P in different chemical forms of *C. indica* and derived hydrochar were presented in Fig. 5. The recovery of P after sequential extraction ranged from 89% to 107%, which evidenced the reliability of the improved sequential phosphorus extraction method in this study. The percentage of H_2O-P in the pristine biomass was up to 67%, much higher than that in sewage sludge (21–26%) (Huang and Tang 2016), animal manure (18–44%) (Huang et al. 2018) and crop straw (25–49%) (Xu et al. 2016). Hence, the direct application of *C. indica* with higher H_2O-P content to soil had a high risk of P loss, which might cause the eutrophication of water. After HTC treatment, the H_2O-P proportion (1–64%) in the derived hydrochars was lower than that in the biomass, reducing the risk of P leaching loss during the

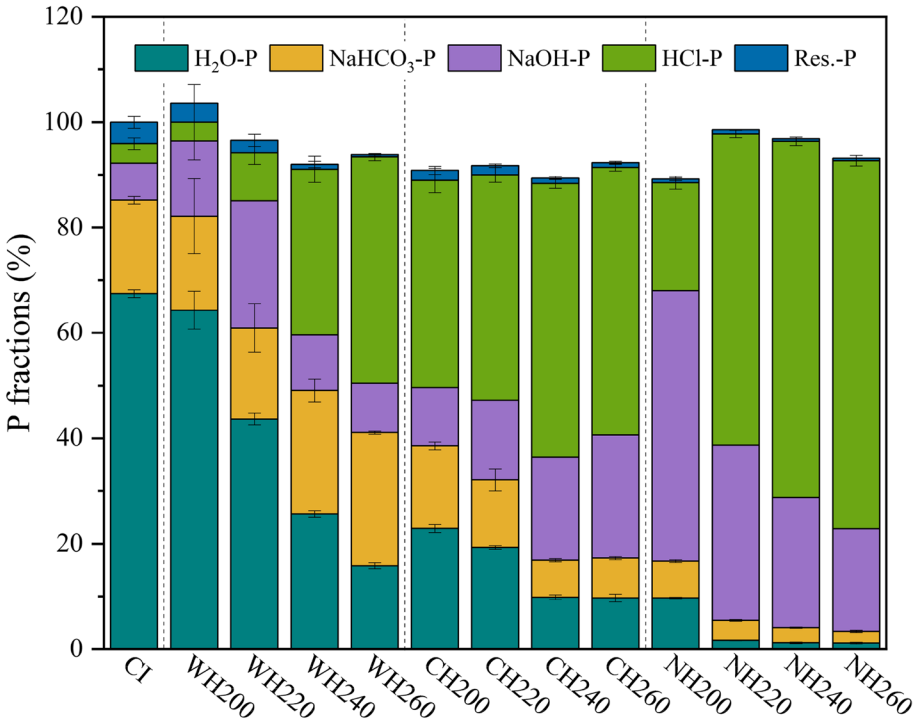


Fig. 5 Distribution of different P pools by sequential extraction of *C. indica* and the derived hydrochars at different temperatures and reaction media. Error bars represent standard deviation observed for triplicate experiments

application of hydrochars. At the same liquid medium, the H_2O-P fraction in hydrochar significantly decreased with increasing temperature ($F_{WHs}=1041.5$, $p<0.01$; $F_{CHs}=10.5$, $p<0.01$; $F_{NHs}=295.5$, $p<0.01$, respectively), implying that the stabilization of P in hydrochar was promoted by HTC temperature. This temperature-dependent trend was in accordance with previously reported HTC of animal manure (Huang et al. 2018) and sewage sludge (Huang and Tang 2016). The addition of $CaCl_2$ and NaOH during HTC process further enhanced the stabilization of P in the hydrochars, especially NH240 and NH260 with only 1% of H_2O-P.

The proportion of $NaHCO_3$-P elevated in WHs but reduced in CHs and NHs compared to that of 17.78% in *C. indica.* With increasing temperature, there was an increase in the proportion of $NaHCO_3$-P in WHs, while a decrease was observed in CHs and NHs. This indicated that some water-soluble phosphorus in the feedstock was converted to less stable P in the HTC process with deionized water as liquid medium and the modification of $CaCl_2$ and NaOH enhanced the complexation of P with the metal, resulting in the less-stable P form decreased with the increase of temperature. The NaOH-P percentage in hydrochars was higher than that of the feedstock, indicating that part of phosphorus would gradually transform into moderately unstable phosphorus during the HTC process. Moreover, it gradually reduced at a certain temperature (220°C-260°C) in the hydrochar derived under deionized water conditions. A similar phenomenon was found in NHs, while the opposite phenomenon was observed in CHs. The content of NaOH-P increased after HTC, indicating the increase of P species formed by the combination of phosphorus and Al/Fe (Qian et al. 2019). After the HTC process, the content of HCl-P in hydrochar elevated with the increasing temperature until HCl-P became the dominant form of phosphorus. HCl-P has been considered to be the calcium/magnesium forms of phosphorus which was the stable form (Xu et al. 2016). Except for the highest percentage of HCl-P in CH200, the proportion of HCl-P in NHs was higher than that in WHs or CHs under the same temperature. The residual phosphorus (Res.-P) in hydrochar was lower than that in *C. indica* (4%), which should be caused by the stable decomposition of organic P (Cui et al. 2020), and a large number of difficult-to-release organic P was converted into inorganic phosphorus and migrated to the liquid phase.

These results indicated that phosphorus in wetland plant was essentially stabilized after HTC, however, the degrees of stabilization varied with temperature and liquid medium. The increase in temperature contributed to the transformation of phosphorus into a more stable phosphorus form, and the change of liquid medium enhanced it. The main chemical form of NHs were NaOH-P and HCl-P (71.82–92.31%), in good agreement with the XANES results. The content of Fe/Al-P determined by XANES was correlated with that of NaOH-P ($r=0.696$, $p<0.01$), and a significant correlation was observed between HAP and HCl-P in hydrochar ($r=0.931$, $p<0.01$). Compared with Al-P and Fe–P, inorganic phosphorus was more likely to combine with calcium, magnesium, and other metals to form stable phosphates such as Ca-P and Mg-P under the condition of higher HTC temperature, abundant Ca^{2+}, and alkaline liquid medium, which was consistent with the P K-edge XANES spectrum analysis mentioned above.

3.3 Characterization of C. indica and the derived hydrochars

3.3.1 Basic characteristics

The fundamental physicochemical properties of *C. indica* and the derived hydrochars were shown in Table 2. The yield of hydrochar varied from 11.43% to 48.70%. With increasing temperature, the yield of hydrochar significantly decreased under the same liquid medium ($F_{WHs}=660.2$, $p<0.01$; $F_{CHs}=469.2$, $p<0.01$; $F_{NHs}=746.0$, $p<0.01$). This is due to the fact that the polymers (such as hemicellulose and cellulose) in the biomass undergo cleavage to produce liquid products and low molecular weight gas phase products such as CO_2, CO, H_2O, and H_2 (Lu et al. 2014) as the temperature increased. The yield of CHs was the highest, followed by WHs and the lowest in NHs at the same temperature. This phenomenon is due to the fact the alkaline condition contributed to the depolymerization of lignocellulose (Wang et al. 2022), while the Ca ions in the process water could be combined with other ions and retained in the hydrochar by adsorption or precipitation (Zheng et al. 2020). The results indicated that temperature and liquid medium were the main factors affecting the yield of hydrochar.

As shown in Table 2, with elevating HTC temperature, the pH of WHs and CHs significantly increased ($F_{WHs}=6238.4$, $p<0.01$; $F_{CHs}=3678.5$, $p<0.01$), while NHs significantly decreased ($F_{NHs}=146.7$, $p<0.01$). After applying HTC with deionized water and $CaCl_2$ solution as liquid medium, the pH of hydrochar and liquid product were acidic, while the pH became alkaline with NaOH solution as HTC liquid medium. The solubilization of alkali metals and the preservation of oxygenated acidic functional groups during the hydrothermal carbonization process (Cui et al. 2022; Irfan et al. 2016), as well as the attachment of organic matter from the liquid medium (Reza et al. 2015), should be responsible for the change on the pH of the hydrochar. At low temperature, cellulose and hemicellulose were usually degraded into simple organic acid products. With the increasing temperature, lignin began to decompose and generate slightly acidic

Table 2 Physicochemical properties of *C. indica* and the derived products at different conditions

Sample	Yield (%)	pH_{HL}[a]	pH_{HC}[b]	Ash (%)	Elemental content (%)				
					C	N	H	O	S
CI			6.51 ± 0.01	15.18 ± 0.30	37.17	1.13	4.74	41.66	0.12
WH200	46.58 ± 0.32a	4.36 ± 0.04d	5.12 ± 0.01d	5.22 ± 0.28c	48.80	1.14	5.22	39.55	0.07
WH220	32.92 ± 0.26b	4.55 ± 0.02c	5.63 ± 0.03c	4.83 ± 0.26c	54.89	1.41	5.23	33.56	0.08
WH240	29.04 ± 0.66c	4.76 ± 0.06b	6.54 ± 0.01b	6.79 ± 0.40b	58.58	1.74	5.20	27.60	0.09
WH260	27.25 ± 0.92d	5.08 ± 0.02a	6.82 ± 0.02a	9.33 ± 0.14a	64.91	2.15	5.36	18.15	0.10
CH200	48.70 ± 0.71a	4.31 ± 0.01d	5.75 ± 0.01d	7.16 ± 0.11b	50.75	1.37	5.21	35.51	0.00
CH220	43.40 ± 0.71b	4.62 ± 0.03c	5.89 ± 0.01c	6.84 ± 0.58b	56.84	1.68	5.18	29.37	0.09
CH240	31.95 ± 0.49c	4.78 ± 0.01b	6.59 ± 0.02b	9.49 ± 0.10a	61.03	1.96	5.00	22.43	0.09
CH260	28.15 ± 1.06d	4.82 ± 0.03a	6.71 ± 0.01a	9.86 ± 0.19a	62.66	2.03	5.05	20.29	0.11
NH200	27.06 ± 0.33a	13.01 ± 0.04a	10.57 ± 0.02a	17.07 ± 0.53d	35.87	0.32	4.87	41.87	0.00
NH220	23.27 ± 0.47b	12.70 ± 0.04b	10.50 ± 0.02b	23.83 ± 0.86c	37.24	0.38	4.98	33.57	0.00
NH240	13.86 ± 0.61c	11.01 ± 0.06c	10.37 ± 0.01c	34.85 ± 0.75b	36.14	0.53	4.54	23.94	0.00
NH260	11.43 ± 0.44d	10.11 ± 0.08d	10.34 ± 0.01c	36.73 ± 0.72a	41.24	0.85	4.43	16.75	0.00

[a] pH_{HL} is the pH of the hydrothermal carbonization liquid product

[b] pH_{HC} is the pH of hydrochar

phenolic substances, coupled with the consumption of organic acids and the formation of ammonium and other alkaline products (Ekpo et al. 2016a), which could explain the increasing pH of hydrochar at higher temperature. As for NaOH-mediated HTC, it was possible that the alkaline liquid medium promoted the leaching of lipids and proteins, and further, the rise in temperature promoted the hydrolysis of macromolecular organic matter in biomass into short-chain fatty acids (Zhang et al. 2022), and the generated acidic liquid products neutralized part of the alkalinity. The pH had a significant effect on the migration of phosphorus between solid and liquid products. Higher pH would inhibit the migration of phosphorus to liquid products and promote the precipitation of phosphorus with cation, facilitating the enrichment of phosphorus in hydrochar, which is evidenced by the significant correlation between the pH value and P recovery rate ($r = 0.813$, $p < 0.01$).

Compared with the ash content of biomass (15.18%), the ash content of WHs and CHs significantly decreased, while the ash content of NHs significantly increased. As opposed to the yield, the ash content significantly elevated with increasing temperature ($F_{WHs} = 152.6$, $p < 0.01$; $F_{CHs} = 73.8$, $p < 0.01$; $F_{NHs} = 494.6$ $p < 0.01$). It is conspicuous that NHs had a low yield from 11.43% to 27.06% and high ash content from 17.07% to 36.73%. This is because HTC promoted the occurrence of demineralization reaction, and the release of organic matter with high boiling point resulted in the accumulation of mineral elements. Acidic liquid medium was conducive to the release of minerals so that the metal ions in biomass transferred to the liquid phase. The alkaline liquid medium inhibited the dissolution behavior of metal ions, which was conducive to the occurrence of precipitation reaction, hence the ash content in hydrochar increased significantly.

With increasing HTC temperature, the content of C and N increased, while the O content decreased, and the H content was relatively stable in the hydrochars (Table 2). The content of N in WHs and CHs was higher than that in the feedstock. It showed that the metal ion Ca^{2+} and higher HTC temperature were favorable for the conversion of N in the liquid to more stable compounds migrating into hydrochars, while the alkaline condition would inhibit it (Ekpo et al. 2016a). As shown in Fig. 6, dehydration and decarboxylation were the major reactions performed during HTC. The H/C and O/C atomic ratios of hydrochar decreased with the increasing reaction temperature with the same liquid medium, suggesting that the aromatic structures and hydrophobic surfaces of hydrochar were enhanced at higher HTC temperature.

3.3.2 Functional groups

The FTIR spectra of the C. indica biomass and the derived hydrochar were depicted in Fig. 7. As shown in the FTIR spectra, the functional groups were effectively preserved on the surface of the hydrochar from *C. indica* biomass by HTC. The functional groups in hydrochar exhibited a distinct temperature-dependent evolution. The characteristic peaks of C-O and C–O–C (1032–1159 cm^{-1}) in WHs and CHs gradually weakened with increasing HTC temperature, indicating the degradation of hemicellulose and cellulose (Dai et al. 2013). The gradual weakening of broad peaks

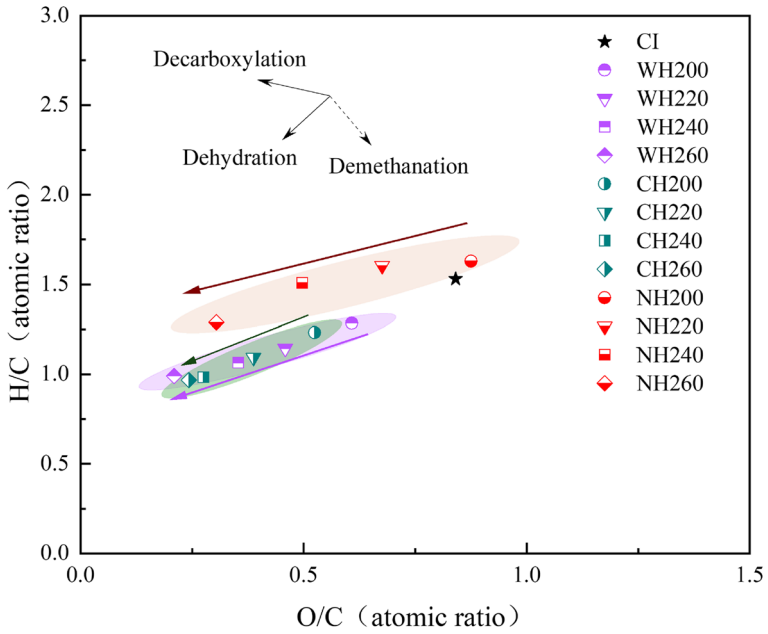


Fig. 6 Van Krevelen diagram of *C. indica* and the derived hydrochars

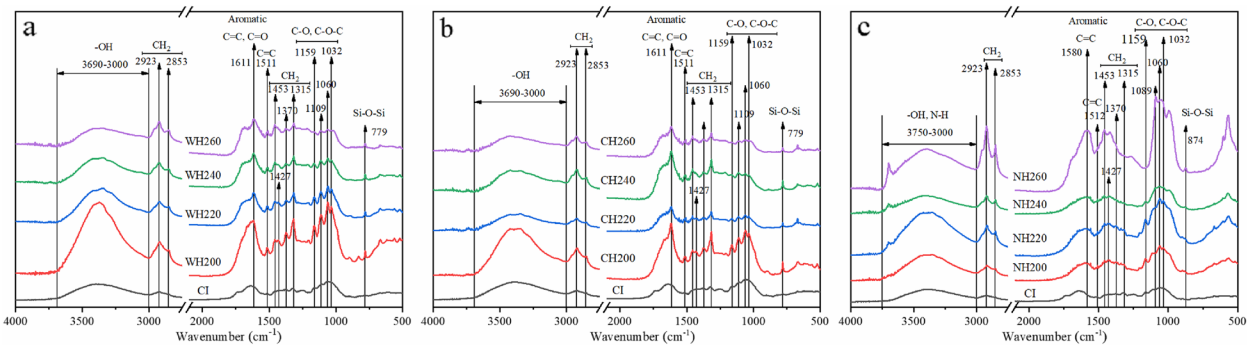


Fig. 7 FTIR spectra and spectroscopic assignment of *C. indica* and the derived hydrochars at different temperatures and reaction media (**a**) H_2O, (**b**) $CaCl_2$ and (**c**) NaOH

around 3400 cm^{-1} suggested a loss of -OH groups in hydrochar due to dehydration reactions (Keiluweit et al. 2010). The C=O and C=C absorption bands weaken around 1611 and 1510 cm^{-1} with increasing temperature due to the catalyzed condensation reaction (Yang et al. 2015). The characteristic peaks of $CaCl_2$-modified hydrochars exhibited a slight reduction in intensity of typical functional groups (e.g., -OH, C-O, and C–O–C) compared to WHs, indicating that $CaCl_2$ could disrupt hydrogen bonding between adjacent cellulose polymer strands (Lynam et al. 2012). Cellulose and hemicellulose underwent further degradation, particularly in the presence of the catalytic salt. However, a more pronounced alteration was observed in NHs, where peak intensities of functional groups (e.g., C-O, and C–O–C) were enhanced. This enhancement could be attributed to an increase in the pH of the liquid medium, which promoted organic matter cleavage and retention of oxygen-containing functional groups (Yang et al. 2015). In comparison with WHs, an obvious shift occurred at the peak of C=C at 1580 cm^{-1} for NHs, belonging to aromatic groups was attributed to the conjugation effect resulting from increased aromatic ring structures (Liu et al. 2024). In summary, different HTC conditions such as temperature, metal ions, and pH of the liquid medium significantly influenced the functional group evolution, resulting in changes of the physicochemical properties of the hydrochar.

3.4 Effect of endogenous-P in hydrochars on soil available P

DGT technique was used to analyze the available P to plants in soil mixed with hydrochar (Fig. 8). The concentration of DGT-P ($C_{DGT\text{-}P}$) in the soil with hydrochar addition (108–201 μg·L^{-1}) was higher than that in the control soil (103 μg·L^{-1}), which indicated that the addition of hydrochar elevated the available P content in soil. Similarly, an increase in soil DGT-P content was found in the application of biochar derived from sludge (Vogel et al. 2017) and animal manure (Bruun et al. 2017). With increasing HTC temperature, the increase in $C_{DGT\text{-}P}$ elevated from 5.00% and 10.30% to 54.00% and 36.84% with the application of WHs and CHs, respectively, suggesting that the available P content in the hydrochar increased with the increasing reaction temperature. As for the hydrochar prepared with NaOH as the liquid medium, the growth rate of soil DGT-P content fluctuated between 39.43% and 55.88% with the rising HTC temperature after applying hydrochar to the soil. Despite the significant increase in the TP content of NHs with increasing temperature, the P species became more stable. This resulted in a fluctuating trend of available P content in NHs. The correlational analysis between DGT-P and $NaHCO_3$/NaOH-P as well as the various P species fitted by linear superposition with P K-edge XANES was carried out. Generally, $NaHCO_3$-P and NaOH-P were considered the potentially available P in soil. As a result, $C_{DGT\text{-}P}$ was correlated with the content of NaOH-P content ($r=0.654$, $p<0.01$), whereas it was not correlated with $NaHCO_3$-P content ($r=0.483$, $p=0.111$) and total contents of NaOH-P and $NaHCO_3$-P ($r=0.337$, $p=0.108$). In contrast, Menezes-Blackburn et al. reported that the correlation between $C_{DGT\text{-}P}$ and $NaHCO_3$-P ($r=0.57$, $p<0.01$) was significant in 32 soils (Menezes-Blackburn et al. 2016). Notably, $C_{DGT\text{-}P}$ was significantly correlated with the Fe/Al-P ($r=0.795$, $p<0.01$) determined by XANES. The Fe/Al-P were demonstrated to be a source of available P for soils (Wu et al. 2014). Hence, DGT-P showed a good agreement with the chemically extracted P and different P species in the assessment of available P in soil, but the specific correspondence varied with the application conditions such as soil properties, biochar type, and climate conditions. Among all the hydrochars, NHs showed the best effect on the $C_{DGT\text{-}P}$ improvement at the same HTC temperature, which could be attributed to higher available phosphorus content in NHs.

Therefore, combining the DGT, XANES, and the chemical extraction results, higher HTC temperature and alkaline modification could improve the P availability of hydrochar during the soil application process, which could provide theoretical support for the target design of the P-enriched hydrochar. Moreover, considering the unique alkaline property of NaOH-modified hydrochar (pH = ~10.5), it has good potential for the improvement of acid soils via pH modification and P promotion. In addition to the P species in hydrochar, the migration and transformation of P during the soil application process should be further determined to achieve the efficient utilization of P.

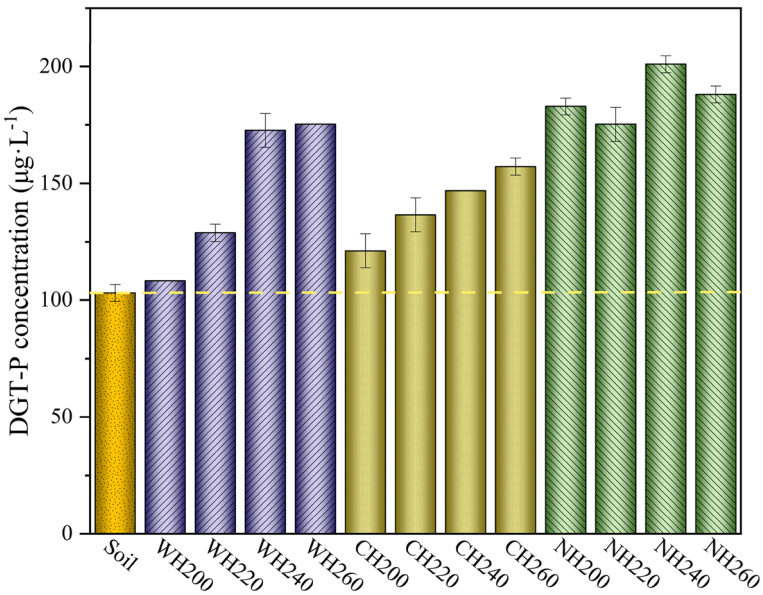


Fig. 8 DGT concentration of P in soil and its mixture with 3% hydrochars. Error bars represent standard deviations observed for triplicate experiments

4 Conclusions

It is essential to elucidate the evolution of phosphorus during hydrothermal carbonization of wetland plants to achieve efficient reclamation and reutilization of phosphorus. This work highlighted the migration and transformation of phosphorus in typical wetland plant during hydrothermal carbonization and further analyzed the effect of endogenous-P in hydrochar on soil available P. The targeted enrichment and 100% recovery of phosphorus in hydrochar were achieved by changing HTC conditions. In general, the enrichment of P in hydrochar was facilitated by elevated temperature, which was further enhanced by metal ions Ca^{2+} and alkaline liquid medium. P K-edge XANES, ^{31}P-liquid NMR, and sequential extraction analyses indicated that temperature, metal ions and the pH of the liquid medium were important in shaping the phosphorus forms. More stable P compounds such as hydroxyapatite dominated in hydrochar with elevating the reaction temperature, addition of exogenous calcium ions, and alkaline medium. Hence, it is possible to regulate the species of phosphorus in hydrochar and achieve efficient recovery by changing the HTC temperature and the liquid medium. The application of hydrochar led to an increase in soil available P content, which was attributed to the abundance of different available endogenous P forms in the hydrochar. Naturally, the fertilization potential of hydrochar still depended on a variety of factors such as soil properties, microbial activity, and climate conditions. Considering that the P in wetland plant biomass was absorbed from wastewater or eutrophic water, the derived hydrochar is a promising shuttle to transfer the surplus P in the water body to P-deficient soil. Moreover, the P-enriched hydrochar from wetland plant could be an alternative phosphorus fertilizer to alleviate the shortage of phosphate ore. Hence, the target design of P-enriched hydrochar from wetland plant via changing the liquid medium and reaction temperature is a promising win–win strategy. Furthermore, future studies are needed to determine the fertilization potential of the P-enriched hydrochar via field trial prior to the large-scale soil application.

Abbreviations

HTC	Hydrothermal carbonization
P	Phosphorus
TP	Total phosphorus
IP	Inorganic phosphorus
OP	Organic phosphorus
XANES	X-ray absorption near edge structure
NMR	Nuclear magnetic resonance
DGT	Diffusive gradients in thin films
WP	Wetland plant
$AlPO_4$	Aluminium phosphate
$FePO_4$	Ferrous phosphate
$MgHPO_4$	Magnesium hydrogen phosphate
$CaHPO_4$	Calcium hydrogen phosphate
$Ca(H_2PO_4)_2$	Monocalcium phosphate
$Ca_3(PO_4)_2$	Calcium phosphate tribasic
HAP	Hydroxylapatite
OCP	Octacalcium phosphate
K_3PO_4	Tripotassium orthophosphate
KH_2PO_4	Potassium dihydrogen phosphate
K_2HPO_4	Dipotassium hydrogen phosphate
LCF	Linear superposition fitting

Supplementary Information

The online version contains supplementary material available at https://doi.org/10.1007/s44246-024-00120-5.

Supplementary Material 1.

Acknowledgements

This work was carried out with the support of 4B7A beamline at Beijing Synchrotron Radiation Facility. And the authors acknowledged the anonymous reviewers for comments to improve the quality of this work.

Authors' contributions

All authors contributed to the study conception and design. Material preparation, data collection and analysis were performed by Fan Yu, Xutong Wang, Yuting Wang, and Zhanjun Cheng. The first draft of the manuscript was written by Junxia Wang and Xiaoqiang Cui. Beibei Yan and Guanyi Chen commented on previous versions of the manuscript. All authors read and approved the final manuscript.

Funding

This study was supported by a grant from National Natural Science Foundation of China (Grant No. 42107237) and National Key Research and Development Program of China (Grant No. 2019YFC1903905).

Availability of data and materials

The datasets used or analyzed during the current study are available from the corresponding author on reasonable request.

Declarations

Competing interests

Guanyi Chen is an editorial board member for Carbon Research and was not involved in the editorial review, or the decision to publish, this article. All authors declare that there are no competing interests.

Author details

[1]School of Environmental Science and Engineering/ Tianjin Key Lab of Biomass Waste Utilization, Tianjin University, Tianjin 300072, China. [2]Institute of Energy and Power Engineering, Zhejiang University of Technology, Hangzhou 310023, China. [3]Nuclear and Radiation Safety Center, MEE, Beijing 100082, China. [4]Tianjin Academy of Eco-Environmental Sciences, Tianjin 300191, China. [5]School of Mechanical Engineering, Tianjin University of Commerce, Tianjin 300134, China.

Received: 28 December 2023 Revised: 24 February 2024 Accepted: 14 March 2024
Published online: 16 April 2024

References

Akbari M, Oyedun AO and Kumar A (2020) Techno-economic assessment of wet and dry torrefaction of biomass feedstock. Energy 207. https://doi.org/10.1016/j.energy.2020.118287.

Babinszki B, Jakab E, Sebestyén Z, Blazsó M, Berényi B, Kumar J, Krishna BB, Bhaskar T and Czégény Z (2020) Comparison of hydrothermal carbonization and torrefaction of azolla biomass: Analysis of the solid products. J Anal Appl Pyrol 149. https://doi.org/10.1016/j.jaap.2020.104844.

Bruun S, Harmer SL, Bekiaris G, Christel W, Zuin L, Hu Y, Jensen LS, Lombi E (2017) The effect of different pyrolysis temperatures on the speciation and availability in soil of P in biochar produced from the solid fraction of manure. Chemosphere 169:377–386. https://doi.org/10.1016/j.chemosphere.2016.11.058

Chen G, Wang J, Yu F, Wang X, Xiao H, Yan B, Cui X (2022) A review on the production of P-enriched hydro/bio-char from solid waste: Transformation of P and applications of hydro/bio-char. Chemosphere 301:134646. https://doi.org/10.1016/j.chemosphere.2022.134646

Chen Q, Sun S, Ran G, Wang C, Gu W, Song Q (2021) Electrochemical detection of phosphate ion in body fluids with a magnesium phosphate modified electrode. Anal Sci 37(9):1247–1252. https://doi.org/10.2116/analsci.20P415

Cui X, Hao H, He Z, Stoffella PJ, Yang X (2016) Pyrolysis of wetland biomass waste: potential for carbon sequestration and water remediation. J Environ Manage 173:95–104. https://doi.org/10.1016/j.jenvman.2016.02.049

Cui X, Lu M, Khan MB, Lai C, Yang X, He Z, Chen G, Yan B (2020) Hydrothermal carbonization of different wetland biomass wastes: Phosphorus reclamation and hydrochar production. Waste Manage 102:106–113. https://doi.org/10.1016/j.wasman.2019.10.034

Cui X, Yang X, Sheng K, He Z, Chen G (2019) Transformation of phosphorus in wetland biomass during pyrolysis and hydrothermal treatment. ACS Sustain Chem Eng 7(19):16520–16528. https://doi.org/10.1021/acssuschemeng.9b03784

Cui XQ, Wang JT, Wang XT, Khan MB, Lu M, Khan KY, Song YJ, He ZL, Yang XE, Yan BB and Chen GY (2022) Biochar from constructed wetland biomass waste: A review of its potential and challenges. Chemosphere 287. https://doi.org/10.1016/j.chemosphere.2021.132259.

Dai L, Tan F, Wu B, He M, Wang W, Tang X, Hu Q, Zhang M (2015) Immobilization of phosphorus in cow manure during hydrothermal carbonization. J Environ Manage 157:49–53. https://doi.org/10.1016/j.jenvman.2015.04.009

Dai Z, Meng J, Muhammad N, Liu X, Wang H, He Y, Brookes PC, Xu J (2013) The potential feasibility for soil improvement, based on the properties of biochars pyrolyzed from different feedstocks. J Soils Sediments 13(6):989–1000. https://doi.org/10.1007/s11368-013-0698-y

Ekpo U, Ross AB, Camargo-Valero MA, Fletcher LA (2016a) Influence of pH on hydrothermal treatment of swine manure: Impact on extraction of nitrogen and phosphorus in process water. Biores Technol 214:637–644. https://doi.org/10.1016/j.biortech.2016.05.012

Ekpo U, Ross AB, Camargo-Valero MA, Williams PT (2016b) A comparison of product yields and inorganic content in process streams following thermal hydrolysis and hydrothermal processing of microalgae, manure and digestate. Biores Technol 200:951–960. https://doi.org/10.1016/j.biortech.2015.11.018

El-Naggar A, Lee SS, Rinklebe J, Farooq M, Song H, Sarmah AK, Zimmerman AR, Ahmad M, Shaheen SM, Ok YS (2019) Biochar application to low fertility soils: a review of current status, and future prospects. Geoderma 337:536–554. https://doi.org/10.1016/j.geoderma.2018.09.034

Ge Z, Wei D, Zhang J, Hu J, Liu Z, Li R (2019) Natural pyrite to enhance simultaneous long-term nitrogen and phosphorus removal in constructed wetland: three years of pilot study. Water Res 148:153–161. https://doi.org/10.1016/j.watres.2018.10.037

Ghanim BM, Kwapinski W, Leahy JJ (2018) Speciation of nutrients in Hydrochar produced from hydrothermal carbonization of poultry litter under different treatment conditions. ACS Sustainable Chemistry & Engineering 6(9):11265–11272. https://doi.org/10.1021/acssuschemeng.7b04768

Gorzelnik SA, Zhu X, Angelidaki I, Koski M, Valverde-Perez B (2023) Daphnia magna as biological harvesters for green microalgae grown on recirculated aquaculture system effluents. Sci Total Environ 873:162247. https://doi.org/10.1016/j.scitotenv.2023.162247

Han X, Wang F, Zhou B, Chen H, Yuan R, Liu S, Zhou X, Gao L, Lu Y, Zhang R (2019) Phosphorus complexation of sewage sludge during thermal hydrolysis with different reaction temperature and reaction time by P K-edge XANES and (31)P NMR. Sci Total Environ 688:1–9. https://doi.org/10.1016/j.scitotenv.2019.06.017

Hao X, Wang C, van Loosdrecht MC, Hu Y (2013) Looking beyond struvite for P-recovery. Environ Sci Technol 47(10):4965–4966. https://doi.org/10.1021/es401140s

Heidari S, Reyhanitabar A, Oustan S (2017) Kinetics of phosphorus desorption from calcareous soils using DGT technique. Geoderma 305:275–280. https://doi.org/10.1016/j.geoderma.2017.06.012

Heilmann SM, Jader LR, Harned LA, Sadowsky MJ, Schendel FJ, Lefebvre PA, von Keitz MG, Valentas KJ (2011a) Hydrothermal carbonization of microalgae II. Fatty acid, char, and algal nutrient products. Applied Energy 88(10):3286–3290. https://doi.org/10.1016/j.apenergy.2010.12.041

Heilmann SM, Jader LR, Sadowsky MJ, Schendel FJ, von Keitz MG, Valentas KJ (2011b) Hydrothermal carbonization of distiller's grains. Biomass Bioenerg 35(7):2526–2533. https://doi.org/10.1016/j.biombioe.2011.02.022

Heilmann SM, Molde JS, Timler JG, Wood BM, Mikula AL, Vozhdayev GV, Colosky EC, Spokas KA, Valentas KJ (2014) Phosphorus reclamation through hydrothermal carbonization of animal manures. Environ Sci Technol 48(17):10323–10329. https://doi.org/10.1021/es501872k

Huang R, Fang C, Zhang B, Tang Y (2018) Transformations of Phosphorus Speciation during (Hydro)thermal Treatments of Animal Manures. Environ Sci Technol 52(5):3016–3026. https://doi.org/10.1021/acs.est.7b05203

Huang R, Tang Y (2016) Evolution of phosphorus complexation and mineralogy during (hydro)thermal treatments of activated and anaerobically digested sludge: Insights from sequential extraction and P K-edge XANES. Water Res 100:439–447. https://doi.org/10.1016/j.watres.2016.05.029

Inyang M, Gao B, Pullammanappallil P, Ding W, Zimmerman AR (2010) Biochar from anaerobically digested sugarcane bagasse. Biores Technol 101(22):8868–8872. https://doi.org/10.1016/j.biortech.2010.06.088

Irfan M, Chen Q, Yue Y, Pang RZ, Lin QM, Zhao XR, Chen H (2016) Co-production of biochar, bio-oil and syngas from halophyte grass (Achnatherum splendens L.) under three different pyrolysis temperatures. Biores Technol 211:457–463. https://doi.org/10.1016/j.biortech.2016.03.077

Kambo HS, Dutta A (2015) A comparative review of biochar and hydrochar in terms of production, physico-chemical properties and applications. Renew Sustain Energy Rev 45:359–378. https://doi.org/10.1016/j.rser.2015.01.050

Keiluweit M, Nico PS, Johnson MG, Kleber M (2010) Dynamic molecular structure of plant biomass-derived black carbon (Biochar). Environ Sci Technol 44(4):1247–1253. https://doi.org/10.1021/es9031419

Li C, Ding SM, Yang LY, Wang Y, Ren MY, Chen MS, Fan XF, Lichtfouse E (2019) Diffusive gradients in thin films: devices, materials and applications. Environ Chem Lett 17(2):801–831. https://doi.org/10.1007/s10311-018-00839-9

Liu WJ, Zeng FX, Jiang H, Yu HQ (2011) Total recovery of nitrogen and phosphorus from three wetland plants by fast pyrolysis technology. Biores Technol 102(3):3471–3479. https://doi.org/10.1016/j.biortech.2010.10.135

Liu XG, Chen YD, Wang H, Yuan SJ and Dai XH (2024) Obtain high quality hydrochar from waste activated sludge with low nitrogen content using acids and alkali pretreatment by enhancing hydrolysis and catalyzation. J Anal Appl Pyrol 177. https://doi.org/10.1016/j.jaap.2023.106315.

Lu X, Flora JR, Berge ND (2014) Influence of process water quality on hydrothermal carbonization of cellulose. Biores Technol 154:229–239. https://doi.org/10.1016/j.biortech.2013.11.069

Lynam JG, Reza MT, Vasquez VR, Coronella CJ (2012) Effect of salt addition on hydrothermal carbonization of lignocellulosic biomass. Fuel 99:271–273. https://doi.org/10.1016/j.fuel.2012.04.035

Menezes-Blackburn D, Zhang H, Stutter M, Giles CD, Darch T, George TS, Shand C, Lumsdon D, Blackwell M, Wearing C, Cooper P, Wendler R, Brown L, Haygarth PM (2016) A Holistic Approach to Understanding the Desorption of Phosphorus in Soils. Environ Sci Technol 50(7):3371–3381. https://doi.org/10.1021/acs.est.5b05395

Osman AI, Zhang Y, Lai ZY, Rashwan AK, Farghali M, Ahmed AA, Liu Y, Fang B, Chen Z, Al-Fatesh A, Rooney DW, Yiin CL, Yap P-S (2023) Machine learning and computational chemistry to improve biochar fertilizers: a review. Environ Chem Lett 21(6):3159–3244. https://doi.org/10.1007/s10311-023-01631-0

Prendergast-Miller MT, Duvall M, Sohi SP (2014) Biochar-root interactions are mediated by biochar nutrient content and impacts on soil nutrient availability. Eur J Soil Sci 65(1):173–185. https://doi.org/10.1111/ejss.12079

Qian T, Yang Q, Jun DCF, Dong F, Zhou Y (2019) Transformation of phosphorus in sewage sludge biochar mediated by a phosphate-solubilizing microorganism. Chem Eng J 359:1573–1580. https://doi.org/10.1016/j.cej.2018.11.015

Qian T, Zhang X, Hu J, Jiang H (2013) Effects of environmental conditions on the release of phosphorus from biochar. Chemosphere 93(9):2069–2075. https://doi.org/10.1016/j.chemosphere.2013.07.041
Reza MT, Rottler E, Herklotz L, Wirth B (2015) Hydrothermal carbonization (HTC) of wheat straw: influence of feedwater pH prepared by acetic acid and potassium hydroxide. Biores Technol 182:336–344. https://doi.org/10.1016/j.biortech.2015.02.024
Robinson JS, Baumann K, Hu Y, Hagemann P, Kebelmann L, Leinweber P (2018) Phosphorus transformations in plant-based and bio-waste materials induced by pyrolysis. Ambio 47(Suppl 1):73–82. https://doi.org/10.1007/s13280-017-0990-y
Sun K, Qiu M, Han L, Jin J, Wang Z, Pan Z, Xing B (2018) Speciation of phosphorus in plant- and manure-derived biochars and its dissolution under various aqueous conditions. Sci Total Environ 634:1300–1307. https://doi.org/10.1016/j.scitotenv.2018.04.099
Tan Z, Lagerkvist A (2011) Phosphorus recovery from the biomass ash: a review. Renew Sustain Energy Rev 15(8):3588–3602. https://doi.org/10.1016/j.rser.2011.05.016
Vaclav S (2000) Phosphorus in the environment: natural flows and human interferences. Ann Rev Energy Environ 25(1):53–88. https://doi.org/10.1146/annurev.energy.25.1.53
Verma S, Murugavel R (2020) Di-tert-butylphosphate Derived Thermolabile Calcium Organophosphates: Precursors for Ca(H(2)PO(4))(2), Ca(HPO(4)), alpha-/beta-Ca(PO(3))(2), and Nanocrystalline Ca(10)(PO(4))(6)(OH)(2). Inorg Chem 59(18):13233–13244. https://doi.org/10.1021/acs.inorgchem.0c01591
Vogel C, Sekine R, Steckenmesser D, Lombi E, Steffens D, Adam C (2017) Phosphorus availability of sewage sludge-based fertilizers determined by the diffusive gradients in thin films (DGT) technique. J Plant Nutr Soil Sci 180(5):594–601. https://doi.org/10.1002/jpln.201600531
Wang W, Zhang L, Li A (2022) Response relationship of hydrothermal humification products of waste biomass withacid-base property of medium. J Dalian Univ Tech 62(01):9–17. https://doi.org/10.7511/dllgxb202201002
Wu Y, Prietzel J, Zhou J, Bing H, Luo J, Yu D, Sun S, Liang J, Sun H (2014) Soil phosphorus bioavailability assessed by XANES and Hedley sequential fractionation technique in a glacier foreland chronosequence in Gongga Mountain. Southwestern China Science China Earth Sciences 57(8):1860–1868. https://doi.org/10.1007/s11430-013-4741-z
Xu G, Zhang Y, Shao H, Sun J (2016) Pyrolysis temperature affects phosphorus transformation in biochar: chemical fractionation and (31)P NMR analysis. Sci Total Environ 569–570:65–72. https://doi.org/10.1016/j.scitotenv.2016.06.081
Yang L, Wu Y, Wang Y, An W, Jin J, Sun K, Wang X (2021) Effects of biochar addition on the abundance, speciation, availability, and leaching loss of soil phosphorus. Sci Total Environ 758:143657. https://doi.org/10.1016/j.scitotenv.2020.143657
Yang W, Shimanouchi T, Kimura Y (2015) Characterization of the Residue and Liquid Products Produced from Husks of Nuts from Carya cathayensis Sarg by Hydrothermal Carbonization. ACS Sustainable Chemistry & Engineering 3(4):591–598. https://doi.org/10.1021/acssuschemeng.5b00103
Yek PNY, Cheng YW, Liew RK, Mahari WAW, Ong HC, Chen WH, Peng WX, Park YK, Sonne C, Kong SH, Tabatabaei M, Aghbashlo M and Lam SS (2021) Progress in the torrefaction technology for upgrading oil palm wastes to energy-dense biochar: A review. Renew Sustain Energy Rev 151. https://doi.org/10.1016/j.rser.2021.111645.
Yu F, Li X, Wang J, Wang X, Xiao H, Wang Z, Cui X, Hu Y, Yan B, Chen G (2022) Coupling anaerobic digestion with pyrolysis for phosphorus-enriched biochar production from constructed wetland biomass. ACS Sustain Chem Eng 10(12):3972–3980. https://doi.org/10.1021/acssuschemeng.1c08537
Zhang J, Wang Y, Wang X, Wu W, Cui X, Cheng Z, Yan B, Yang X, He Z, Chen G (2022) Hydrothermal conversion of Cd/Zn hyperaccumulator (Sedum alfredii) for heavy metal separation and hydrochar production. J Hazard Mater 423(Pt B):127122. https://doi.org/10.1016/j.jhazmat.2021.127122
Zheng X, Jiang Z, Ying Z, Ye Y, Chen W, Wang B, Dou B (2020) Migration and Transformation of Phosphorus during Hydrothermal Carbonization of Sewage Sludge: Focusing on the Role of pH and Calcium Additive and the Transformation Mechanism. ACS Sustain Chem Eng 8(21):7806–7814. https://doi.org/10.1021/acssuschemeng.0c00031
Zheng X, Shen M, Ying Z, Feng Y, Wang B, Dou B (2022) Correlating phosphorus transformation with process water during hydrothermal carbonization of sewage sludge via experimental study and mathematical modelling. Sci Total Environ 807(Pt 1):150750. https://doi.org/10.1016/j.scitotenv.2021.150750

Publisher's Note

Springer Nature remains neutral with regard to jurisdictional claims in published maps and institutional affiliations.